Journal of Hazardous Materials 177 (2010) 539–545

Contents lists available at ScienceDirect

Journal of Hazardous Materials

journal homepage: www.elsevier.com/locate/jhazmat

Bioreduction of trivalent aurum to nano-crystalline gold particles by active and inactive cells and cell-free extract of *Aspergillus oryzae* var. *viridis*

A.R. Binupriya[a], M. Sathishkumar[b,*], K. Vijayaraghavan[b], S.-I. Yun[a,*]

[a] *Department of Food Science and Technology, College of Agriculture and Life Science, Chonbuk National University, Jeonju 561-756, Republic of Korea*
[b] *Singapore-Delft Water Alliance, National University of Singapore, 2 Engineering Drive 2, Singapore 117577, Singapore*

ARTICLE INFO

Article history:
Received 25 August 2009
Received in revised form
17 November 2009
Accepted 14 December 2009
Available online 22 December 2009

Keywords:
Aspergillus oryzae var. *viridis*
Active and inactive biomass
Cell-free extract
Bioreduction
Gold nanoparticles

ABSTRACT

Bioreduction efficacy of both active (AB) and inactive (IB) cells/biomass of *Aspergillus oryzae* var. *viridis* and their respective cell-free extracts (ACE and ICE) to convert trivalent aurum to gold nanoparticles were tested in the present study. Strong plasmon resonance of gold nanoparticles was observed between 540 and 560 nm in the samples obtained from AB, IB, ACE and ICE. Transmission electron microscopy (TEM), field emission scanning electron microscopy (FE-SEM), energy dispersive X-ray (EDX) and X-ray diffraction (XRD) were performed to examine the formation of gold nanoparticles. Comparing all four forms of *A. oryzae* var. *viridis*, ICE showed high gold nanoparticle productivity. The nanoparticles formed were quite uniform in shape and ranged in size from 10 to 60 nm. In addition some triangle, pentagon and hexagon-shaped nanoplates with size range of 30–400 nm were also synthesized especially at lower pH. Organics from the inactive cells are believed to be responsible for reduction of trivalent aurum to nano-sized gold particles. Organic content of the ICE was found to be double the amount of ACE. High productivity of gold nanoparticles by metabolic-independent process opens up an interesting area of nanoparticle synthesis using waste fungal biomass from industries.

© 2009 Elsevier B.V. All rights reserved.

1. Introduction

Nanoscience and technology has grabbed attention from all fields of science due to the innumerable applications of nanoparticles. Currently the potential application of nano-scale matter in nanocomputers, synthesis of advanced materials, energy storage devices, electronic and optical displays, chemical and biosensors as well as biomedical devices is being explored [1]. Especially gold nanoparticles find a wide application in various fields. The most widespread and common synthesis of gold nanoparticles is the chemical reduction of a ionic gold in aqueous phase by a chemical reducing agent such as $NaBH_4$, citrate, and ascorbate. Small and monodispersed gold nanoparticles were synthesized using strong reductant such as borohydride. But such reducing agents may be associated with environmental toxicity or biological hazards, where as comparatively safer reductants like citrate, ascorbate, simple sugars like glucose, fructose etc. were not efficient in productivity. It has been, therefore, of increasing interest to develop efficient green synthesis of gold nanoparticles. In addition most of these physical and chemical methods need extreme conditions like temperature, pressure etc. In recent years, there is lot of interest shown in the environmentally benign synthesis of nanoparticles that do not use any toxic chemicals or extreme conditions in the synthesis process. Many biological systems such as that of fungi [2,3], algae [4,5], bacteria [6,7], actinomycetes [8], and plants [9–11] have been studied for biosynthesis of gold and silver nanoparticles. Synthesis of nanoparticles may be intracellular or extracellular of which the later is more preferred as it makes the downstream processing less laborious and also is effective in cost-cutting of the entire process during industrial applications. When compared to bacteria, fungi are more suitable of extracellular synthesis due to their large biomass which enables easy handling during biosynthesis. But not many studies on inactive cells and cell-free extract of fungi for gold nanoparticles synthesis are available. Gold nanoparticles (Au NPs) have potentially exciting applications in hyperthermia of tumors, optical coatings and scanning tunneling microscopes as conductive tips [12]. The possible wide applications of Ag and Au NPs and the need to synthesize these particles in nano-size under most non-toxic eco-friendly conditions has led many researchers to search for suitable biological systems for their biosynthesis.

In the present study *Aspergillus oryzae* var. *viridis* an economically important fungus was used for both intracellular and extracellular synthesis of Au NPs. *A. oryzae* var. *viridis* is an economically important fungus in food industries. It plays a major role in the

Abbreviations: AB, active biomass; IB, inactive biomass; ACE, active cell extract; ICE, inactive cell extract; Au NPs, gold nanoparticles.

* Corresponding authors. Tel.: +65 6 5165844.
E-mail addresses: cvemuthu@nus.edu.sg, sathishkumar77@gmail.com (M. Sathishkumar), siyun@chonbuk.ac.kr (S.-I. Yun).

0304-3894/$ – see front matter © 2009 Elsevier B.V. All rights reserved.
doi:10.1016/j.jhazmat.2009.12.066

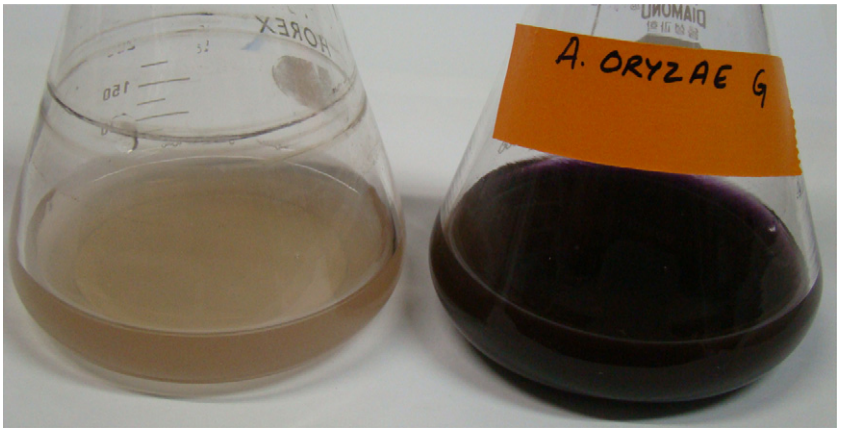

Fig. 1. Visible color change of the ICE-$HAuCl_4$ mixture after 120 h incubation.

production of rice koji in Japan. This fungus is known to produce a variety of enzymes such as amylases, proteases, protyrosinase, acid carboxypeptidase and urease among the other enzymes. *A. oryzae* var. *viridis* is not known to produce aflatoxins. Though this fungus finds an important place in food industries, it is not studied for its reduction potential of metals. So for the first time we explored the possibility of trivalent aurum reduction to nano-crystalline particles using the live and dead cells of this fungus as well as the cell-free extract/cell filtrates from these cells. Kinetics of synthesis of NPs and the characteristics of the Au NPs were analyzed by various techniques.

2. Materials and methods

2.1. Biomass and cell-free extract production

A. oryzae var. *viridis* (KCCM: 11372) used to make rice Koji in Japan was purchased from Korean Culture Centre for Microorganisms, Seoul, Republic of Korea. For production of biomass, the organism was grown aerobically in sterile liquid media containing (g/l): KH_2PO_4, 7.0; K_2HPO_4, 2.0; $MgSO_4{\cdot}7H_2O$, 0.1; $(NH_4)_2SO_4$, 1.0; yeast extract, 0.6; and glucose, 10.0. The flasks were inoculated and incubated on orbital shaker at 25 °C and 150 rpm. The biomass was harvested after 72 h of growth by sieving through a plastic sieve, followed by extensive washing with sterile deionized water (DI) to remove any medium component from the biomass. All the above procedures were conducted in aseptic condition using sterile containers. Thus obtained biomass was termed as active biomass/cells (AB). Inactive biomass/cells (IB) was prepared by re-suspending the active cells in sterile DI water and suspension was autoclaved at 15 psi and 121 °C for 15 min followed by centrifugation at 8000 rpm for 15 min. The resulting inactive biomass was washed with sterile DI water to separate them from the other media components. Typically 20 g of active and inactive biomass (fresh weight) was brought in contact with 200 ml of sterile Milli-Q DI water separately for 72 h at 25 °C in an Erlenmeyer flask and agitated in the same condition as described earlier. After incubation, the active and inactive cell filtrates were obtained from respective cells by passing it through Whatman filter paper no. 1.

2.2. Biosynthesis of nanoparticles

For synthesis of gold nanoparticles, 0.5 g (fresh weight) of active or inactive biomass was suspended in 50 ml of prepared 1 mM $HAuCl_4$ solution. In case of cell-free extract, 1 mM final concentration of $HAuCl_4$.aq was mixed with 50 ml of cell-free extract from active (ACE) and inactive biomass (ICE) in a 250 ml Erlenmeyer flask and agitated at 150 rpm and 25 °C. Control (only 1 mM $HAuCl_4$.aq and without biomass or cell-free extract) was also run along with the experimental flask. Sample of 1 ml was withdrawn at different time intervals and the absorbance was measured at a resolution of 1 nm using UV–vis spectrophotometer (Shimadzu, UV-1601). After 72 h of incubation the gold nanoparticles formed were analyzed by transmission electron microscopy (TEM) (HITACHI-JP/H7600, Japan) by forming gold nanoparticles film on carbon coated copper TEM grids at a voltage of 100 kV. After the completion of the experiments the reaction mixture was centrifuged at 15,000 rpm for 15 min and the supernatant was collected to analyze the residual ionic gold to check the gold nanoparticles productivity. The ionic gold was analyzed in ICP (Agilent, 7500).

Synthesis of Au NPs at various pH (4–8) was also studied. Initial pH was adjusted using 0.1N HCl or NaOH. Similarly the effect of initial trivalent aurum concentration on Au NPs productivity was tested by varying the initial trivalent aurum concentration from 0.1 mM to 1 mM. The Au NPs synthesized thereby was subjected to further characterization as mentioned earlier.

2.3. Zeta potential, EDX and XRD measurement

Measurements of zeta potential were carried out using Zetasizer Nano ZS (Malvern) and titrator MPT-2. An aqueous suspension of gold nanoparticles was filtered through 0.45 μm PTFE membrane before measurement. The zeta potential was calculated using the Henry's equation. The formation of nanoparticles prepared was examined under vacuum combined with energy dispersive X-ray spectroscopy (EDX) (JEOL JSM-5410LV) and X-ray diffractograms using D/Max 2005, Rigaku.

2.4. FTIR

The gold nanoparticles (0.01 g) dried overnight at 60 °C was mixed with 0.1 g of KBr and pressed into a tablet form by pressing the ground mixed material with the aid of a bench press. The resulting pellet was transparent and was used to test the surface functional groups by IR spectroscopy (Shimadzu 8201PC, Japan) where it was scanned between 4000 and 400 cm^{-1} at a resolution of 4 cm^{-1} in transmittance mode.

3. Results and discussion

3.1. Biosynthesis of gold nanoparticles

The biomasses (AB and IB) and cell-free extracts (ACE and ICE) of *A. oryzae* var. *viridis* were used for the synthesis gold nanopar-

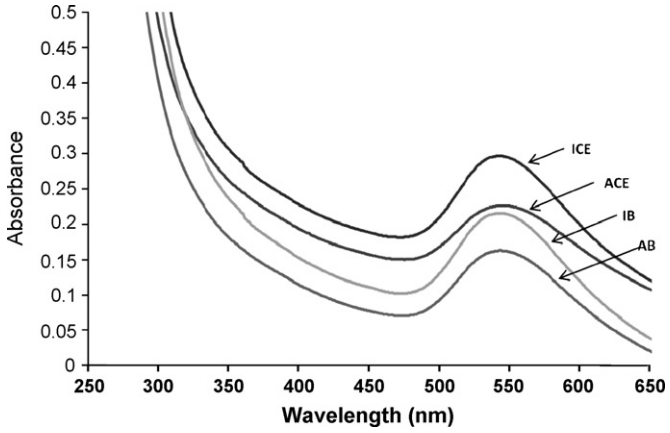

Fig. 2. UV–vis spectra of gold nanoparticles after 120 h incubation (temperature: 25 °C; pH 7 ± 0.2; rpm: 150; initial $HAuCl_4$ concentration: 1 mM).

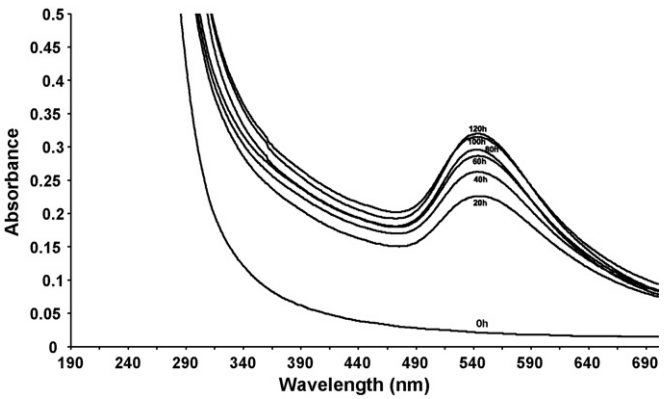

Fig. 3. UV–vis spectra of gold nanoparticles by ICE at various incubation times (temperature: 25 °C; pH 7 ± 0.2; rpm: 150; initial $HAuCl_4$ concentration: 1 mM).

ticles from $HAuCl_4$.aq. The color change of the reaction mixture (Biomass/cell-free extract and chloroaurate solution) on formation of gold nanoparticles was quite evident from the formation of reddish purple from colorless/straw colored reaction mixture (Fig. 1). This color change from colorless/straw color to purple was noticed within the first 10 h of reaction time in the case of both biomasses and cell-free extracts. This visibly confirms the presence of gold nanoparticles in the solution and that $AuCl_4^-$ ions have been reduced to Au^- ions [4,13,14]. The formation and stability of the reduced gold nanoparticles in the colloidal solution was monitored by using UV–vis spectral analysis. The color of the solution remained unaltered even after 3 months without settling in case of ACE and ICE. But in case of AB and IB, color intensity was darker around the biomasses which got settled down. This shows that the nanoparticles formed were mostly concentrated around the biomasses.

3.2. Surface plasmon of Au NPs

An UV–vis spectrum is one of the important techniques to ascertain the formation of metal nanoparticle, provided surface plasmon resonance exists for the metal. UV–vis spectra pattern from all the four biomaterial used (AB, IB, ACE and ICE) were similar. Increase in time increased the intensity of the peak. But on any given time, the peak intensity was high in order of ICE > ACE > IB > AB. Fig. 2 shows the UV–vis spectrum of the various reaction mixtures studied after 120 h of incubation, which indicates the larger peak area for ICE. This shows that the Au NPs productivity was higher in ICE, comparatively. In addition, the residual ionic gold concentration analysis in ICP showed lower ionic gold concentration, which indirectly confirms that ICE produced more Au NPs. The UV–vis spectra recorded from ICE and $HAuCl_4$ reaction mixture at different time intervals of reaction are plotted as shown in Fig. 3. The time at which the aliquots were removed for analysis is indicated next to the respective curves. It was observed from the spectra that the gold surface plasmon resonance band occurs at about 540 nm [6] and this absorption steadily increases in intensity as function of time of reaction. The interaction of light having wavelength smaller than the particles size of Au NPs leads to polarization of the free conduction electrons with respect to the much heavier ionic core of Au NPs. Therefore, an electron dipolar oscillation is created and surface plasmon (SP) absorption band is obtained [15]. The maximum absorption peak was observed at about 554 nm after 120 h incubation time. The red shift from 540 nm for gold NP to 554 nm may be attributed to particle size. The chemically prepared Au NPs has a characteristic band at 520 nm corresponding to 40 nm particle size [16]. Husseiny et al. [16] reported a strong correlation between the particle size and the maximum absorption peak. They found that as the particle size increases the maximum absorption and found to be red shifted. Consequently, the Au NPs prepared by *A. oryzae* var. *viridis* were found to be red shifted, in comparison with that prepared chemically. Basavaraja et al. [17] observed that the red shift, broadening and splitting of the SPR was probably due to the dampening of the surface plasmon resonance caused by the change in the refractive index of the surrounding medium and also increase in the particle size of the silver nanoparticles in colloidal solution. Even after three months, the peak remained close to 555 nm, in the case of ACE and ICE. This indicated that the nanoparticles were well dispersed and that there was not much aggregation.

As mentioned earlier, the color intensity of the reaction mixture was high for IB and ICE. The peak area and height of the UV–vis spectrum obtained for the IB and ICE was also higher compared their counterparts, which confirms the higher productivity of gold nanoparticles. It was assumed that this higher productivity could be attributed to the higher organic content (as reducing agents) present in the inactive cells due to autoclaving. To confirm the presumption, total organic carbon (TOC) was analyzed for both the active and inactive biomasses. The results indicated that the ACE contained 1834 mg/L of TOC and the ICE contained 3613 mg/L, which is almost twice the amount of the former. This result clearly illustrates that autoclaving leads to a release of organics from the cells due to the rupturing of the cell walls.

Similar to surface plasmon study at various time intervals, experiments were also conducted at different initial $HAuCl_4$ concentration keeping the initial biomaterial (ICE) concentration constant. Increase in $HAuCl_4$ concentration increased the intensity of the peak constantly (Fig. 4), which shows that concentration

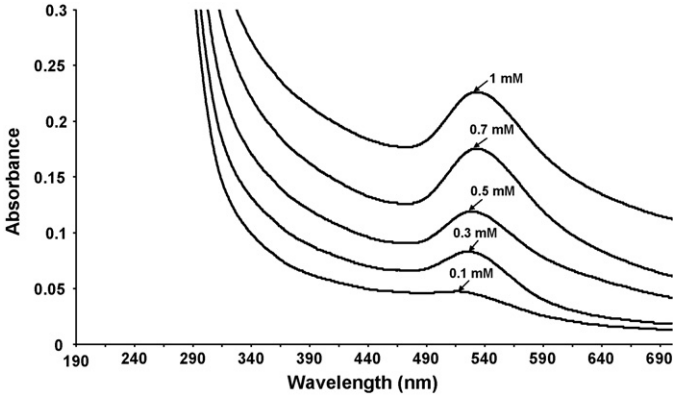

Fig. 4. UV–vis spectra of gold nanoparticles by ICE at various initial $HAuCl_4$ concentrations (temperature: 25 °C; pH 7 ± 0.2; rpm: 150; incubation time: 24 h).

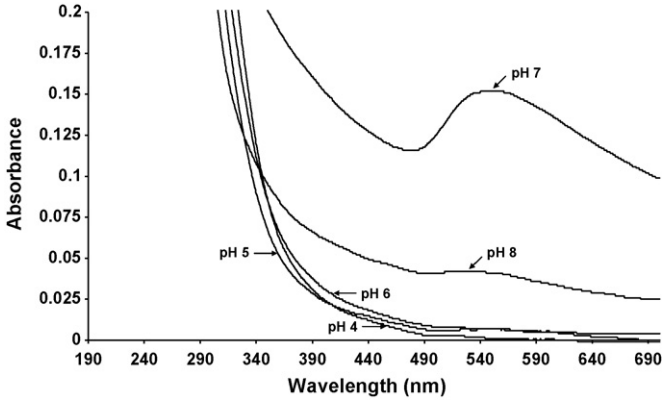

Fig. 5. UV–vis spectra of gold nanoparticles by ICE at various initial pH (temperature: 25 °C; rpm: 150; incubation time: 15 h).

have significant effect on the Au NPs productivity. The same pattern was noticed for all the biomaterials studied. But biomaterial concentration did not affect the morphology of the Au NPs produced. Whereas, it was noticed that increase in initial $HAuCl_4$ concentration had some effect on size of the Au NPs synthesized. Higher initial $HAuCl_4$ concentration facilitated formation of smaller nanoparticles. This could be due to the availability of more ionic gold present in higher initial $HAuCl_4$ concentrations for the reducing agents to convert them to nano-sized zero valent Au particles.

Surface plasmon resonance studies of Au NPs at various pH clearly indicates the formation of Au NPs at neutral pH (Fig. 5). In acidic pH, the formation was almost negligible (Fig. 5). Mild productivity was noticed at pH 8. This shows that acidic pH is not favorable for Au NPs production. Agnihotri et al. [18] reported a similar result for production of Au NPs by marine yeast, *Yarrowia lipolytica* where acidic pH did not favor Au NPs synthesis much but more number of larger-sized crystalline gold triangles and hexagons than near-spherical particles were observed compared to other pH. He et al. [6] reported a similar result for Au NPs synthesis by *Rhodopseudomonas capsulata* at lower pH. At higher pH the particles were mostly spherical and were smaller in size compared to that at acidic pHs. At low pH, the aggregation of Au nanoparticles to form larger nanoparticles was believed to be favoured over the nucleation to form new nanoparticles, whereas at higher pH, however, the large number of functional groups available for gold binding facilitated a higher number of Au^{3+} to bind and subsequently form a large number of nanoparticles with smaller diameters [10]. Thus the very important role played by pH in controlling the shape and size of the Au NPs synthesis is evident from these results. Zeta potential studies for the synthesized Au NPs at various pH conditions showed absolute negative values. It was maximum for the Au NP in colloidal solution synthesized at pH 7. This also indirectly shows the higher productivity of Au NPs at neutral pH. Sathishkumar et al. [10] showed high absolute negative value for Ag NPs synthesized using *Cinnamon* bark extract, which increased with increase in pH.

3.3. TEM, FE-SEM, EDX and XRD measurements

Transmission electron microscopy (TEM) analysis was carried out after 120 h of reaction for all the four biomaterials used (AB, IB, ACE and ICE). TEM measurements show the various shapes and sizes of gold nanoparticles formed by various biomaterials used (Fig. 6). A well-separated triangular and spherical (also rare pentagonal and hexagonal) gold nanoparticles with occasional aggregation are seen in particles formed in ACE and ICE. In case of AB and IB the particles are seen almost embedded on the periphery of fungal cell. This shows that the gold ions are first adsorbed on the fungal mycelium by electrostatic attraction/ion-exchange mechanism and later reduced by either enzymes or organics present in the biomaterial (AB and IB). Fungal cells are known to adsorb the cationic and anionic metal ions on its cell surface through functional groups [19–21]. The particles appear to be thin and transparent as

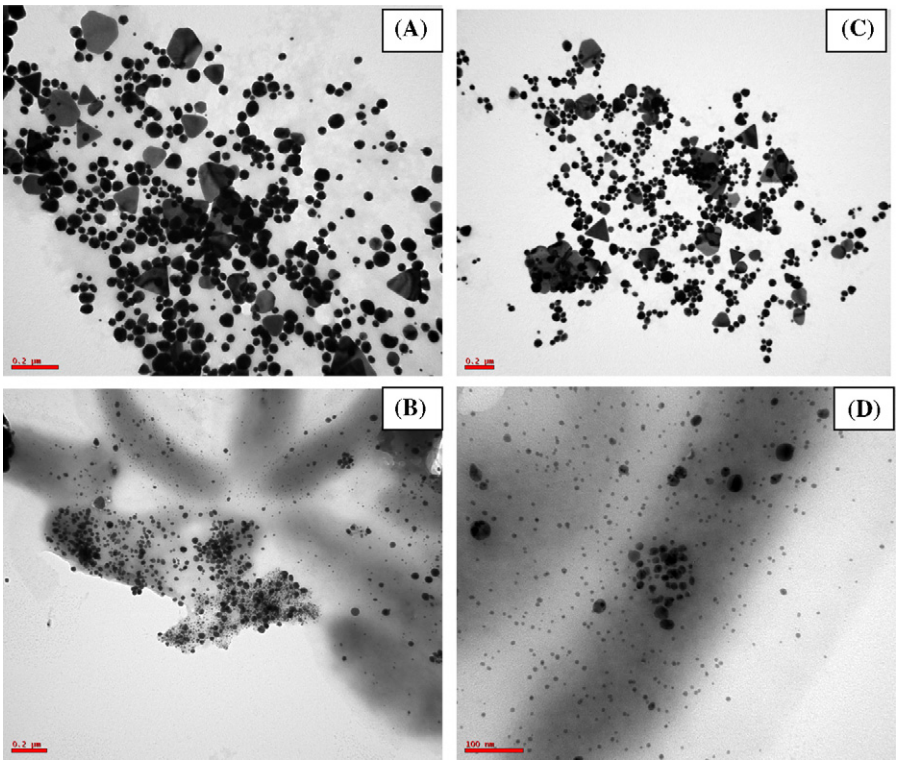

Fig. 6. TEM images of the gold nanoparticles synthesized by (A) ICE, (B) IB, (C) ACE and (D) AB (bar scale: 0.2 μm for A–C; 100 nm for D).

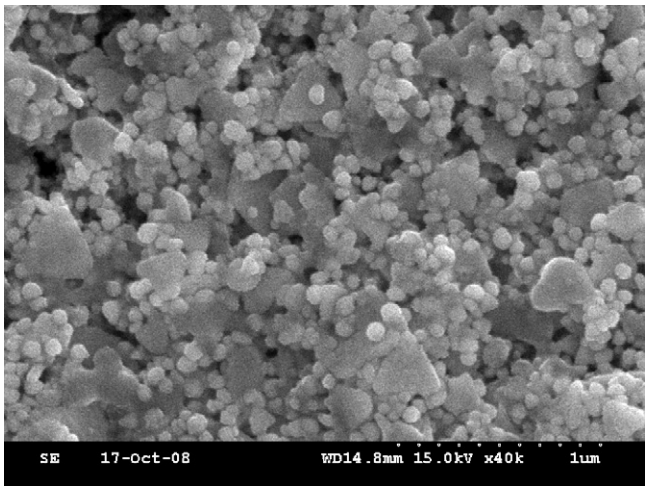

Fig. 7. FE-SEM image of the gold nanoparticles synthesized by ICE (bar scale: 1 μm).

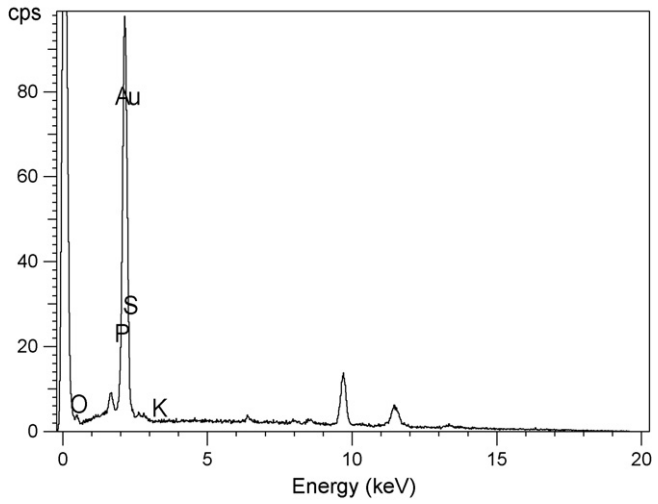

Fig. 8. Energy dispersive X-ray spectrum of gold nanoparticles synthesized by ICE.

apparent from the TEM micrographs. The Au NPs appear to be in various stages of growth. Very large triangular nanoplates appear to have been formed along with small triangular particles. The particle sizes varied from very small (10 nm) to very large particles (400 nm). The average size of nanoparticles synthesized ranged between 30 and 40 nm incase of spherical particles, whereas for triangles, pentagons and hexagons, the average size ranged between 90 and 100 nm. Cell-free extracts (ACE and ICE) produced more triangles, pentagons and hexagons than the biomass (AB and IB). This shows that exudates (either enzymes or organics) from the cell are responsible for the formation of triangle, pentagon and hexagon-shaped nanoparticles. Some congregated nanoparticles were also noticed which could be due to formation of a matrix by ACE and ICE that is seen to hold few particles together. The organic nature of the cell-free extract might result in capping of the particles which in turn might provide stability to the Au NPs formed. Shankar et al. [22] deduced that the reduction of the metal ions is possibly facilitated by reducing sugars and/or terpenoids present in the neem leaf broth; while Singaravelu et al. [4] contributed the stabilization of nanoparticles to the presence of extracellular polysaccharides in seaweed *Sargassum wightii*. To know the morphology of the synthesized nanoparticles better, FE-SEM image was recorded (Fig. 7). It clearly depicted the spherical and triangular-shaped nanoparticles. It also showed the agglomerated nanoparticles in certain places.

The particles were verified using EDX analysis to ensure the presence of Au as shown in Fig. 8. The EDX spectrum also shows that 92.3% was gold. The peak at 2 keV can be assigned to Au NPs and the other peaks may be from the capping agents originated from the fungus present on the surface of the Au NPs. The weak signals of O arise from proteins/enzymes that are either bound to the Au NP or at the vicinity of the particle. At natural conditions around pH 7, the zeta potential of gold nanoparticles synthesized by *A. oryzae* var. *viridis* was −445.62 (mV). Sathishkumar et al. [10] showed high absolute negative value for Ag NPs synthesized using *Cinnamon* bark extract, which increased with increase in pH. At alkaline pH the particles were observed to be stable and dispersed due to electrostatic repulsion. The phase of the prepared nanoparticles was investigated by X-ray diffraction technique and corresponding XRD patterns are shown in Fig. 9. The synthesized Au NPs have shown clear peaks of cubic phases (JCPDS No. 03-0921) at 38.1 (1 1 1), 44.4 (2 0 0), 64.8 (2 2 0) and 77.6 (3 1 1). In addition, some minor peaks representing the hexagonal phases (JCPD No. 41-1402) at 45.9 (1 0 0), 57.9 (1 0 3), 71.6 (0 0 6) and 76.1 (1 0 5) were also noticed. It suggests that the prepared gold nanoparticles are biphasic in nature. The slight shift in the peak positions indicated the presence of strain in the crystal structure which is a characteristic of nanocrystallites. The broad bottom area of the peaks indirectly represents the smaller size of the nanoparticles. Thus the XRD pattern proves to be strong evidence in favor of the UV–vis spectra and TEM images for the presence of gold nanocrystals [13,18,23].

3.4. FTIR

Fig. 10 shows the FTIR spectrum of the Au NPs formed in AB, IB, ACE and ICE after 120 h reaction time. No major difference was noticed in the peak pattern between the biomaterials used other than the peak intensity. Steepness of the peaks represents the differences in the quantity of the representative functional groups [24]. Two bands are seen at 1660 and 1530 cm^{-1}. These bands may be assigned to the amide I and II bands of proteins, respectively. It is well known that proteins can bind to gold nanoparticles either through free amine groups or cysteine residues in the proteins and therefore, stabilization of the gold nanoparticles by surface-bound proteins is a possibility [1,25,26]. These observations are indicative of the binding of protein with Au nanoparticles through free carboxylate group [11]. The bands due to the bending of C–OH and asymmetric stretching of C–O–C groups [27] of protein/polysaccharide appearing as very strong bands in gold nanoparticles further supports this. Mata et al. [5] described that

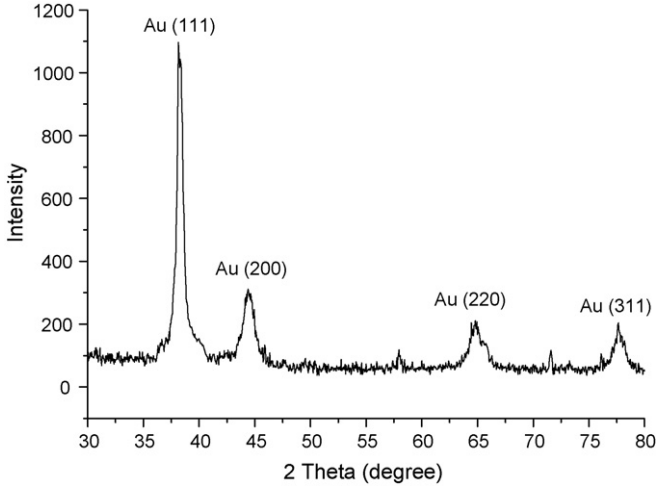

Fig. 9. X-ray diffraction spectrum of gold nanoparticles synthesized by ICE.

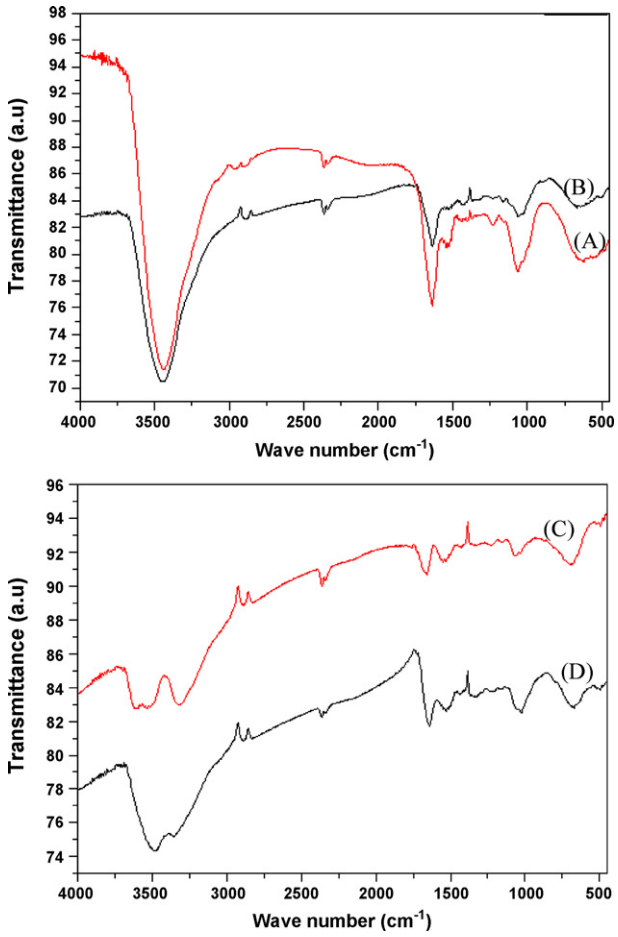

Fig. 10. FT-IR spectrum of gold nanoparticles synthesized by (A) AB, (B) IB, (C) ACE and (D) ICE.

hydroxyl groups (OH) are very abundant in polysaccharides which are majorly responsible for reduction process. They also observed a significant displacement of the CO stretching of COH from 1075 to 1113 cm^{-1} in post-reduction FTIR spectra. The same phenomena would fit well for the present reduction process too. The bands between 3500 and 3300 cm^{-1} are reported to occur due to amine group stretching vibrations superimposed on the side of hydroxyl group band [28,29]. The intensity of these bands was high in the biomass compared to cell filtrates and the pattern is slightly varied.

4. Conclusion

The active and inactive cells/biomass (AB and IB) and their corresponding cell-free extracts (ACE and ICE) of *A. oryzae* var. *viridis* were found to be suitable agents for the synthesis of gold nanoparticles from gold chloride solution. The formation of gold nanoparticles (Au NPs) was visually confirmed by the change in the color of reaction medium from colorless to purple. The Au NPs synthesized were monitored via UV–vis spectrophotometer and characterized. The SPR (Surface Plasmon Resonance) showed the formation of Au NPs with respect to time, pH and initial biomaterial concentration. The peak area of UV–vis spectrum showed that the IB and ICE were found to synthesize more nanoparticles compared to their counterparts, which is believed to be due to presence of more organics in the autoclaved cells due to cell-rupture. High organic content in ICE was confirmed through TOC analysis. The TEM images of formed Au NPs showed that the particles were aggregated and entrapped in some regions possibly an organic matrix of fungal origin. The TEM micrographs of gold nanoparticles formed in cell-free extracts showed polydiversity in shape and size. The particles formed were of different sizes as well as shapes. Particles of very small size of 10 nm as well of large triangular nanoplates of nearly 400 nm were formed in ACE. High pH favored more number of spherical particles, whereas acidic pH did not favor the synthesis of Au NPs. The presence of zero valent gold nanoparticles was confirmed by EDX and XRD measurements. The results show that *A. oryzae* var. *viridis* is a suitable candidate for the synthesis of gold nanoparticles. Other interesting result was the formation of high amount of Au NPs in autoclaved cells and extracts which indicate the role of organics other than enzymes in the reduction reaction. The autoclaved fungal-mediated green chemistry approach towards the synthesis of nanoparticles has many advantages such as ease with which the process can be scaled up, economic viability, simple downstream processing and easy handling of biomass. Compared to bacterial fermentations, in which the process technology involves the use of sophisticated equipment for getting clear filtrates from the colloidal broths, fungal broths can be easily filtered by filter press or similar simple equipment, thus saving considerable investment costs for equipment. The capacity of fungi to produce high amounts of biomass than bacteria make them preferred candidates for nanoparticle synthesis studies.

Acknowledgements

This research was partly supported by Chonbuk National University Post-Doctoral Research fund (2008) and partly by Research Center for Industrial Development of BioFood Materials in Chonbuk National University, Jeonju, Korea. The center is designated as a Regional Innovation Center appointed by the Ministry of Knowledge Economy (MKE), Jeollabuk-do Provincial Government and Chonbuk National University. The authors thank Mr. Jong-Gyun Kang, EM Lab, Center for University-wide research facilities, Chonbuk National University, Korea for TEM analysis.

References

[1] M. Sastry, A. Ahmad, M.I. Khan, R. Kumar, Biosynthesis of metal nanoparticles using fungi and actinomycete, Curr. Sci. 85 (2003) 162–170.
[2] K.C. Bhainsa, S.F. D'Souza, Extracellular biosynthesis of silver nanoparticles using the fungus *Aspergillus fumigatus*, Colloids Surf. B Biointerface 47 (2006) 160–164.
[3] S. Senapati, A. Ahmad, M.I. Khan, M. Sastry, R. Kumar, Extracellular biosynthesis of bimetallic Au–Ag alloy nanoparticles, Small 1 (2005) 517–520.
[4] G. Singaravelu, J.S. Arockiamary, V.G. Kumar, K. Govindaraju, A novel extracellular synthesis of monodisperse gold nanoparticles using marine alga, *Sargassum wightii* Greville, Colloids Surf. B Biointerface 57 (2007) 97–101.
[5] Y.N. Mata, E. Torres, M.L. Blázquez, A. Ballester, F. González, J.A. Muñoz, Gold(III) biosorption and bioreduction with the brown alga *Fucus vesiculosus*, J. Hazard. Mater. 166 (2009) 612–618.
[6] S.Y. He, Z.R. Guo, Y. Zhang, S. Zhang, J. Wang, N. Gu, Biosynthesis of gold nanoparticles using the bacteria *Rhodopseudomonas capsulata*, Mater. Lett. 61 (2007) 3984–3987.
[7] R. Shahverdi, S. Minaeian, H.R. Shahverdi, H. Jamalifar, A.-A. Nohi, Rapid synthesis of silver nanoparticles using culture supernatants of Enterobacteria: a novel biological approach, Proc. Biochem. 42 (2007) 919–923.
[8] A. Ahmad, P. Mukherjee, S. Senapati, D. Mandal, M.I. Khan, R. Kumar, M. Sastry, Extracellular biosynthesis of silver nanoparticles using the fungus *Fusarium oxysporum*, Colloids Surf. B Biointerface 28 (2003) 313–318.
[9] M. Sathishkumar, K. Sneha, I.S. Kwak, J. Mao, S.J. Tripathy, Y.-S. Yun, Phyto-crystallization of palladium through reduction process using *Cinnamon zeylanicum* bark extract, J. Hazard. Mater. 171 (2009) 400–404.
[10] M. Sathishkumar, K. Sneha, S.W. Won, C.-W. Cho, S. Kim, Y.-S. Yun, *Cinnamon zeylanicum* bark extract and powder mediated green synthesis of nano-crystalline silver particles and its bactericidal activity, Colloids Surf. B: Biointerface 73 (2009) 332–338.
[11] S.S. Shankar, A. Ahmad, M. Sastry, Geranium leaf assisted biosynthesis of silver nanoparticles, Biotechnol. Prog. 19 (2003) 1627–1631.
[12] S.S. Shankar, A. Rai, A. Ahmad, M. Sastry, Controlling the optical properties of lemongrass extract synthesized gold nanotriangles and potential application in infrared-absorbing optical coatings, Chem. Mater. 17 (2005) 566–572.
[13] K.B. Narayanan, N. Sakthivel, Coriander leaf mediated biosynthesis of gold nanoparticles, Mater. Lett. 62 (2008) 4588–4590.
[14] Y. Wang, X. He, K. Wang, X. Zhang, W. Tan, *Barbated Skullcup* herb extract-mediated biosynthesis of gold nanoparticles and its primary appli-

cation in electrochemistry, Colloids Surf. B: Biointerface 73 (2009) 75–79.
[15] S. Link, M.A. El-Sayed, Shape and size dependence of radiative, nonradiative, and photothermal properties of gold nanocrystals, Int. Rev. Phys. Chem. 19 (2000) 409.
[16] M.I. Husseiny, M.A. El-Aziz, Y. Badr, M.A. Mahmoud, Biosynthesis of gold nanoparticles using *Pseudomonas aeruginosa*, Spectrochi. Acta Part A 67 (2007) 1003–1006.
[17] S. Basavaraja, S.D. Balaji, A. Lagashetty, A.H. Rajasab, A. Venkataraman, Extracellular biosynthesis of silver nanoparticles using the fungus *Fusarium semitectum*, Mater. Res. Bull. 43 (2008) 1164–1170.
[18] M. Agnihotri, S. Joshi, A.R. Kumar, S. Zinjarde, S. Kulkarni, Biosynthesis of gold nanoparticles by the tropical marine yeast *Yarrowia lipolytica* NCIM 3589, Mater. Lett. 63 (2009) 1231–1234.
[19] A.R. Binupriya, M. Sathishkumar, K. Swaminathan, E.S. Jeong, S.E. Yun, S. Pattabi, Biosorption of metal ions from aqueous solution and electroplating industry wastewater by *Aspergillus japonicus:* phytotoxicity studies, Bull. Environ. Contam. Toxicol. 77 (2006) 219–227.
[20] K.K. Deepa, M. Sathishkumar, A.R. Binupriya, G.S. Murugesan, K. Swaminathan, S.E. Yun, Sorption of Cr(VI) from dilute solutions and wastewater by live and pretreated biomass of *Aspergillus flavus*, Chemosphere 62 (2006) 833–840.
[21] M. Sathishkumar, A.R. Binupriya, K. Swaminathan, J.G. Choi, S.E. Yun, Bioseparation of toxic arsenate ions from dilute solutions by native and pretreated biomass of *Aspergillus fumigatus* in batch and column mode: effect of biomass pretreatment, Bull. Environ. Contam. Toxicol. 81 (2008) 316–322.
[22] S.S. Shankar, A. Rai, A. Ahmad, M. Sastry, Rapid synthesis of Au, Ag, and bimetallic Au core–Ag shell nanoparticles using Neem (*Azadirachta indica*) leaf broth, J. Colloid Interface Sci. 275 (2004) 496–502.
[23] D. Philip, Biosynthesis of Au, Ag and Au–Ag nanoparticles using edible mushroom extract, Spectrochim. Acta Part A 73 (2009) 374–381.
[24] A.R. Binupriya, M. Sathishkumar, C.S. Ku, S.I. Yun, Sequestration of reactive blue 4 by free and immobilized *Bacillus subtilis* cells and its extracellular polysaccarides, Colloids Surf. B: Biointerface, in press.
[25] A. Gole, C. Dash, V. Ramachandran, A.B. Mandale, S.R. Sainkar, M. Rao, M. Sastry, Pepsin–gold colloid conjugates: preparation, characterization and enzyme activity, Langmuir 17 (2001) 1674–1679.
[26] N. Vigneshwaran, A.A. Kathe, P.V. Varadarajan, R.P. Nachane, R.H. Balasubramanya, Silver–protein (core–shell) nanoparticle production using spent mushroom substrate, Langmuir 23 (2007) 7113–7117.
[27] S. Li, Y. Shen, A. Xie, X. Yu, X. Zhang, L. Yang, C. Li, Rapid room-temperature synthesis of amorphous selenium/protein composites using *Capsicum annuum* L. extract, Nanotechnology 18 (2007) 405101.
[28] A. Saeeda, M. Iqbala, S.I. Zafarb, Immobilization of *Trichoderma viride* for enhanced methylene blue biosorption: batch and column studies, J. Hazard. Mater. 168 (2009) 406–415.
[29] M.Y. Arica, G. Bayramoglu, Biosorption of Reactive Red 120 dye from aqueous solution by native and modified fungus biomass preparations of *Lentinus sajorcaju*, J. Hazard. Mater. 149 (2007) 499–507.